

Crystallization Kinetics of Palm Stearin in Blends with Sesame Seed Oil

J.F. Toro-Vazquez*, M. Briceño-Montelongo, E. Dibildox-Alvarado, M. Charó-Alonso, and J. Reyes-Hernández

Centro de Investigación y Estudios de Posgrado de la Facultad de Ciencias Químicas, Universidad Autónoma de San Luis Potosí, San Luis Potosí, SLP, 78210, México

ABSTRACT: This study investigates the crystallization kinetics of palm stearin (PS), a palm oil fraction, in blends with sesame seed oil. The results indicate that the crystallization behavior of PS in sesame oil is mainly associated with the crystallization of tripalmitin. Therefore, crystallization of blends of 26, 42, 60, and 80% (wt/vol) PS in sesame oil was described by equations developed for simpler systems (e.g., Fisher and Turnbull equation). The isothermal crystallization, melting profile, and fitting of the kinetics of nucleation to the Fisher and Turnbull equation showed that the 26, 42, and 60% PS/sesame oil blends crystallized mainly in the β_1' polymorph state. In contrast, the 80% blend crystallized in two different polymorph states (i.e., β_1' at $T \leq 307.6$ K and β_1 at $T \geq 308.2$ K). The data indicated that, in spite of the higher concentration of PS in the 80% PS/sesame oil system, crystallization in the β_1 state required more free energy for nucleation (ΔG_c) than β_1' crystallization in the 26, 42, and 60% PS/sesame oil. At the low cooling rate used (1 K/min) it was observed that, for a particular PS blend, the higher the effective supercooling the higher the viscosity of the oil phase and the smaller the induction time of crystallization (τ_i). Additionally, the β_1' crystals from PS, developed at the highest effective supercooling investigated, were smaller than the β_1 crystals obtained at lower effective supercooling.

Paper no. J9235 in *JAOCs* 77, 297–310 (March 2000).

KEY WORDS: Avrami, crystallization, Fisher-Turnbull, oil viscosity, palm oil, palm stearin.

Sesame (*Sesamum indicum* L.) is an important annual oilseed crop in developing countries. India, China, Sudan, Mexico, and Burma produced approximately 60% of its global production for the period 1987–1991 (1,2). Sesame oil, conventionally extracted by pressing roasting seeds without further refining, has a mild, pleasant, and unique taste with remarkable oxidative stability. The fatty acid composition, triacylglyceride distribution, concentrations of sterols, tocopherols and lignins in the oil, and the effect of several processing conditions on its oxidative stability have been studied (1,3–7).

*To whom correspondence should be addressed at Facultad de Ciencias Químicas-CIEP, Universidad Autónoma de San Luis Potosí, Av. Dr. Manuel Nava 6, Zona Universitaria, San Luis Potosí, SLP 78210, México.
E-mail: toro@uaslp.mx

Nowadays consumers are demanding edible oils devoid of any chemical treatment and with natural characteristics and natural flavor. As a consequence, the market for novel oils that are cold-press extracted and that possess natural oxidative stability has been developing worldwide during the last few years. Sesame seed oil fulfills most of these characteristics and is now marketed in industrialized countries, mainly as a gourmet salad oil with unique flavor. However, additional value-added products like margarine, spreads, and squeezable spreads based on sesame oil have not been developed. These products require a solid-to-liquid ratio with the appropriate melting profile to obtain the texture and functionality (i.e., spreadability) desired by consumers. However, the natural triglyceride composition of sesame oil is highly unsaturated, consisting of 7–12% palmitic, 3.5–6% stearic, 0.09–0.29% palmitoleic, 39–43% oleic, 40–44% linoleic, and 0.40–0.85% linolenic acids (1,8). Using differential scanning calorimetry (DSC), Dibildox-Alvarado and Toro-Vazquez (8) determined the crystallization exotherm for triglycerides in sesame oil with an onset at around -2.5°C and a maximum at around -7°C . Thus, the development of a functional solid phase in sesame oil without the use of chemical processes, such as hydrogenation and interesterification, is not an easy task.

Several processes are used to modify the phase change properties of vegetable oils and improve their plasticity, and therefore, the versatility for use by the food industry. The most utilized processes are hydrogenation and interesterification (9). However, hydrogenation of the naturally occurring *cis* unsaturated fatty acids (i.e., oleic, linoleic, and linolenic fatty acids) produces *trans* fatty acids. Consumer concern associated with the atherogenic effects of *trans* fatty acids limits the future of this process as a way to modify the solid-to-liquid ratio in vegetable oils. In fact, more *trans*-free spreads (e.g., obtained without hydrogenation) are being introduced successfully into the market. This trend is expected to continue as the proposal of the U.S. Food and Drug Administration to specify *trans* fatty acid content in food product labels proceeds (10). On the other hand, chemical or enzymatic interesterification processes, technologies utilized mainly in European countries, have particular drawbacks that are mainly associated with the yield efficiency and cost of the processes (11). In these processes, a high-melt-

ing temperature fraction [i.e., palm stearin (PS), full or partially hydrogenated oils] is interesterified with a particular vegetable oil in the manufacture of *trans*-free margarine and vegetable shortening (12,13).

An additional alternative involves the direct blending of a high-melting temperature fraction with a vegetable oil (i.e., sesame oil). This last process has the additional advantage that no chemical process is involved, consistent with the consumer trend toward natural products. The aim of this study was to investigate the crystallization kinetics of PS, a palm oil fraction constituted mainly by triglycerides of high-melting temperature, in blends with sesame seed oil. This process constitutes a feasible alternative to expand the use of sesame oil through the development of value-added products such as squeezable margarines, spreads, or low-fat margarines. According to the National Association of Margarine Manufacturers, the consumption of margarine-type products grew from 2.6 to 9.1 pounds per capita for the period between 1930 and 1996 (10). In contrast, butter consumption dropped from 17.6 to 4.3 pounds per person (10).

PS is obtained through fractional crystallization of refined, bleached, and deodorized palm oil (12). Tripalmitin (TP) is the triglyceride with the highest melting temperature in both palm oil (5–10% w/w) and PS (12–56% w/w), depending on the fractionation temperature (14). As a consequence, TP should affect crystallization kinetics and polymorphic behavior of palm oil and PS. Our previous research (8,15) on crystallization has indicated that solutions of pure TP in sesame oil behave like binary solutions formed by saturated triglycerides (i.e., TP) and unsaturated triglycerides (i.e., sesame oil). In the present study, we evaluate whether this behavior holds in a more complex crystallization system, i.e., mixtures of PS in sesame oil.

MATERIALS AND METHODS

Materials. Whole-seed refined sesame oil was obtained from a local company (DIPASA de México, Celaya, Gto., México). The oil was stored at 4°C in the dark. The same batch was used in all the experiments.

Pure TP (>99% pure, experimentally confirmed by gas chromatography and DSC) was obtained from Sigma Chemical Co. (St. Louis, MO). Refined, bleached, and deodorized PS was provided by the Palm Oil Research Institute of Malaysia (Kuala Lumpur, Malaysia). Both TP and PS were used without further purification.

Chemical analysis. The fatty acids composition of sesame oil and PS was determined by gas chromatography utilizing a Shimadzu chromatograph GC-9A (Shimadzu Corp., Kyoto, Japan) with flame-ionization detector and a Supelco (Bellefonte, PA) glass column (2.6 m × 2.1 mm) packed with GP 10% SP 2330 on Chromosorb 100/120. The analysis conditions have been previously reported (8).

The triglyceride profile for PS was determined by high-performance liquid chromatography (HPLC) following the conditions described previously by Che Man *et al.* (14) utilizing a

Waters 600 E instrument (Waters Millipore Co., Milford, MA) with a refractive index detector and a Nova Pack C₁₈ column (3.9 × 300 mm) (Water Millipore Co.). Triglyceride peaks were assigned based on the retention time of triglyceride standards.

The particular concentration of TP in PS was determined by gas chromatography of the saturated triglyceride fraction isolated by silver ion thin-layer chromatography (TLC) following the conditions described by Nikolova-Damyanova (16)

DSC. A PerkinElmer differential scanning calorimeter (model DSC-7; PerkinElmer, Norwalk, CT) equipped with a dry box was used in all cases. The temperature calibration of the equipment was done with indium (onset temperature for melting = 429.8 K) and *n*-hexatriacontane (onset temperature for melting = 349.3 K), and the baseline was developed with an empty aluminum pan. The calibration for heat involved in phase changes (i.e., melting/crystallization) was made only with indium (ΔH for melting = 28.45 J/g).

Nonisothermal DSC analysis. For dynamic runs, ≈12 mg of TP solution in sesame oil (0.00, 0.32, 0.98, 1.80, 2.62, 10, and 25% wt/vol) or PS blend in sesame oil (0.00, 26, 42, 60, and 80% wt/vol) was sealed in a pan and held at 353 K for 30 min before each DSC scan. The system was cooled at a rate of 10 K/min until a temperature of 243 K was achieved. After 2 min at this temperature, the melting curve was obtained by heating the system at 5 K/min until reaching 353 K. The temperature in the maxima of both the exothermal peak of crystallization (T_{Cr}) and the endothermal melting peak (T_s) were calculated using the DSC-7 software library. In the same way, the heating and cooling thermograms of pure TP and PS were determined.

The ideal behavior of the TP crystallization/melting in both systems, TP/sesame oil and PS/sesame oil, was evaluated using the Hildebrand equation (17):

$$\ln(x) = \Delta H_f / R (1/T_s - 1/T_p) \quad [1]$$

where ΔH_f is the enthalpy of fusion per mole of pure TP, T_p and T_s are the melting temperature of pure TP and in the oil solutions, respectively (i.e., the temperature in the peak maximum in the DSC endotherm), x is the mole fraction of TP in the system (i.e., TP/sesame oil and PS/sesame oil solutions), and R is the universal gas constant. An average molecular weight for sesame oil triglycerides (874.93) and PS triglycerides (842.15) was calculated from the fatty acid composition.

Isothermal DSC analysis. The PS/sesame oil solution (26, 42, 60, and 80% wt/vol) was heated at 353 K for 30 min and then cooled (1.0 K/min) to a preset temperature (297.5–309 K) and held at that temperature for crystallization. After complete crystallization, the system was left at the isothermal temperature for additional 35 min. Afterward, the melting thermogram was obtained by heating the system at a rate of 1.0 K/min. The induction time for crystallization (T_i) was calculated from the isothermal thermogram as the time from the start of the isothermal process to the beginning of crystallization (i.e., time where the heat capacity of the sample had a significant departure from the baseline) using the DSC-7 software library. The cooling rate was selected according to conditions used in previous stud-

ies involving isothermal (8) and nonisothermal (15) TP crystallization in sesame oil. This cooling rate is in line with the slow cooling rate achieved by industrial crystallizers.

Microscopy studies. Crystal morphology of the PS/sesame oil solution was obtained under the same isothermal conditions utilized in the DSC studies using a polarized microscope with camera (model BX60F/PMC35; Olympus Optical Co., Ltd., Tokyo, Japan). The experimental setup has been described previously (8). After induction of nucleation, pictures of the crystals were taken as a function of time.

Calculation of kinetic parameters. The isothermal DSC data were utilized to evaluate the kinetics of TP crystallization in the PS/sesame oil solutions using the Avrami equation (18):

$$-\ln(1 - F) = zt^n \quad [2]$$

where F is the fraction of crystal transformed at time t , n is the index of the crystallization reaction or Avrami exponent, and z is the rate constant of crystallization, which depends on the magnitude of n , the nucleation rate, and the linear growth rate of the spherulite (19). The value of F was calculated by integration of the isothermal DSC crystallization curves as described by Henderson (20) utilizing Equation 3 and according to Figure 1:

$$F = \Delta H_t / \Delta H_{\text{tot}} \quad [3]$$

where ΔH_t is the area under the DSC crystallization curve from $t = T_1$ to $t = t$, and ΔH_{tot} is the total area under the crystallization curve. The values of ΔH_t and ΔH_{tot} were calculated with the DSC software library. In fact, F is a reduced crystallinity since it associates an instant crystallinity to the total one achieved

under the experimental conditions. Then, F varies from 0 to 1.

The value of n was calculated from the slope of the linear regression of the plot of $\ln[-\ln(1 - F)]$ vs. $\ln(t)$ using values of fractional crystallization between 0.25 and 0.75 (18). The n value describes the crystal growth mechanism. Thus, a crystallization process with a $n = 4$ follows a polyhedral crystal growth mechanism, a value of $n = 3$ represents a plate-like crystal growth mechanism, and a $n = 2$ indicates a linear crystal growth (19).

When nucleation occurs from the melt the rate of nucleation, J , depends on the activation free energy to develop a stable nucleus, ΔG_c , and the activation free energy for molecular diffusion, ΔG_d . The Fisher-Turnbull equation (Eq. 4) describes this situation and was utilized, according to Ng (21) and Herrera *et al.* (22), to evaluate the magnitude of ΔG_c

$$J = (NkT/h)\exp(-\Delta G_c/kT)\exp(-\Delta G_d/kT) \quad [4]$$

where J is the rate of nucleation that is inversely proportional to T_1 , N is the number of molecules per mole, k is the Boltzmann constant, T is absolute temperature, and h is Planck's constant. In a spherical nucleus, ΔG_c is associated with the effective supercooling, ΔT , and the surface free energy at the crystal/melt interface, σ , through the following equation:

$$\Delta G_c = (16/3)\pi\sigma^3(T_M^0)^2/(\Delta H)^2(\Delta T)^2 \quad [5]$$

where $(16/3)\pi$ results from the spherical shape attributed to the nucleus and ΔH is the heat of fusion. The effective supercooling, $(T_M^0 - T)$, is the difference between the equilibrium melting temperature, T_M^0 , and the isothermal temperature of crystallization, T . The magnitude of T_M^0 was established following

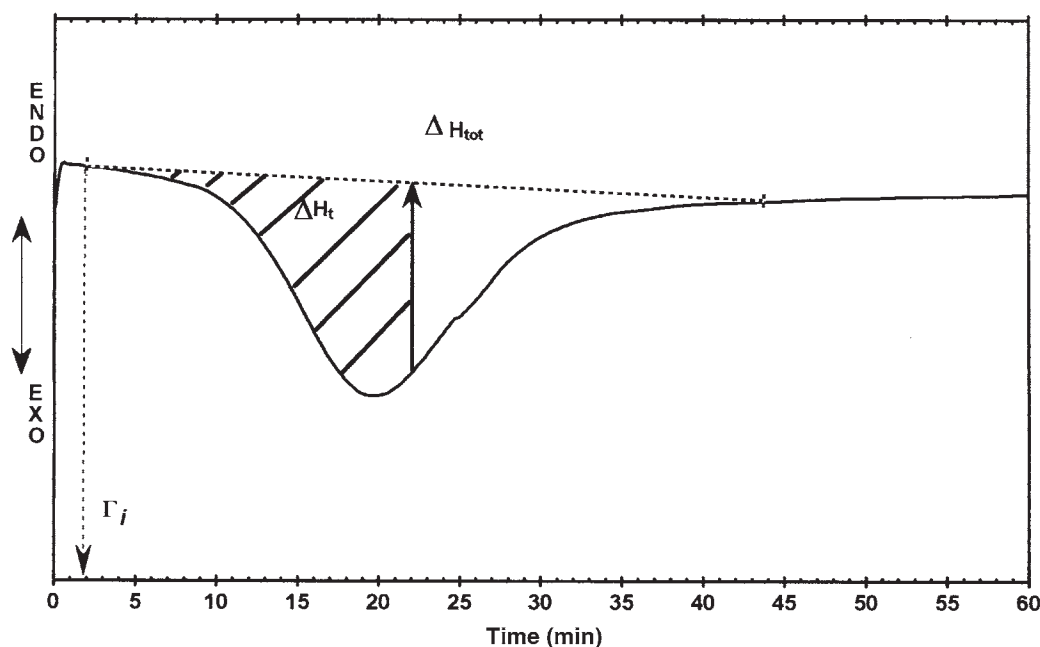


FIG. 1. Determination of reduced crystallinity, F , from exotherm obtained at isothermal conditions.

the procedure described by Hoffman and Weeks (23). Thus, the relationship between T and the apparent melting temperature of TP in the PS/sesame oil solutions (T_M') was established plotting T_M' vs T . The T_M' value was determined from the melting thermograms (heating rate of 1 K/min) after the corresponding crystallization according to the isothermal conditions described previously. Thus, the experimental T_M' vs. T plot provided a straight line whose crossing point with the line $T_M' = T$ represented T_M^o (Fig. 2). The T_M^o value is defined as the temperature where the smallest aggregation of molecules (i.e., unstable crystal nucleus) is in equilibrium with the molecules in the melt. This concept is particularly utilized in polymers (24). Thus, small aggregations of molecules without the correct tridimensional arrangement to develop a stable crystal nucleus will melt below T_M^o . Finally, from the slope, s , of the linear regression of $\log[\tau_1 T]$ vs. $1/T(\Delta T)^2$ the calculation of ΔG_c was performed since $\Delta G_c = s k/(\Delta T)^2$.

Measurements of viscosity. The viscosity of the PS/sesame oil solution was determined under isothermal conditions at a shear rate of 15.82 s^{-1} utilizing a Brookfield LVDV-III viscosimeter (Brookfield Instruments, Stoughton, MA) with a cone and plate geometry with the cup CP-41. In all cases the volume of the sample was 0.5 mL and the temperature control was $\pm 0.1 \text{ K}$ (Brookfield TC-500).

The solution in the sample container of the viscosimeter was heated at 353 K for 30 min. Afterward, the system was cooled (1.0 K/min) until the desired temperature was achieved. The equilibrium time for the recording of the viscosity was 25 s.

The value of viscosity for each PS/sesame oil solution was plotted as a function of the effective supercooling and the τ_1 .

RESULTS AND DISCUSSION

The fatty acid profile of the sesame oil and PS used are presented in Table 1. As previously indicated, sesame seed oil has a high degree of unsaturation, mainly provided by the high concentrations of oleic and linoleic fatty acids.

The triglyceride composition of PS was as follows, where M = myristic, P = palmitic, L = lauric, O = oleic, and St = stearic: MMM, 0.16 ± 0.01 ; MMP, 0.14 ± 0.01 ; MPL, 1.47 ± 0.11 ; PPP, 16.46 ± 0.17 ; PPO, 36.91 ± 0.12 ; PPSt, 3.39 ± 0.06 ; POSt, 31.21 ± 0.03 ; StOSt, 0.06 ± 0.02 ; OOO, 8.00 ± 0.11 ; and unknown, $1.58 \pm 0.77 \text{ wt}\%$. That is, the main constituents of PS were, in decreasing order of concentration, PPO, POSt, PPP, and PPSt, with TP as the triglyceride with the highest melting temperature (14,25). Thus, TP must affect the crystallization kinetics and polymorphic behavior of the PS/sesame oil solutions in a significant way. From the concentration of TP in the PS (16.46%), the effective TP concentrations for the 26, 42, 60, and 80% PS/sesame oil solutions were 4.27, 6.90, 9.85, and 13.14% (wt/vol), respectively.

The corresponding DSC cooling (Fig. 3) and heating (Fig. 4) dynamic thermograms pointed out the high degree of unsaturation of sesame oil. Sesame oil had a crystallization peak with a maximum at $\approx 256 \text{ K}$, a melting peak with maximum at $\approx 258.5 \text{ K}$, and melting was completed at $\approx 266 \text{ K}$. Although,

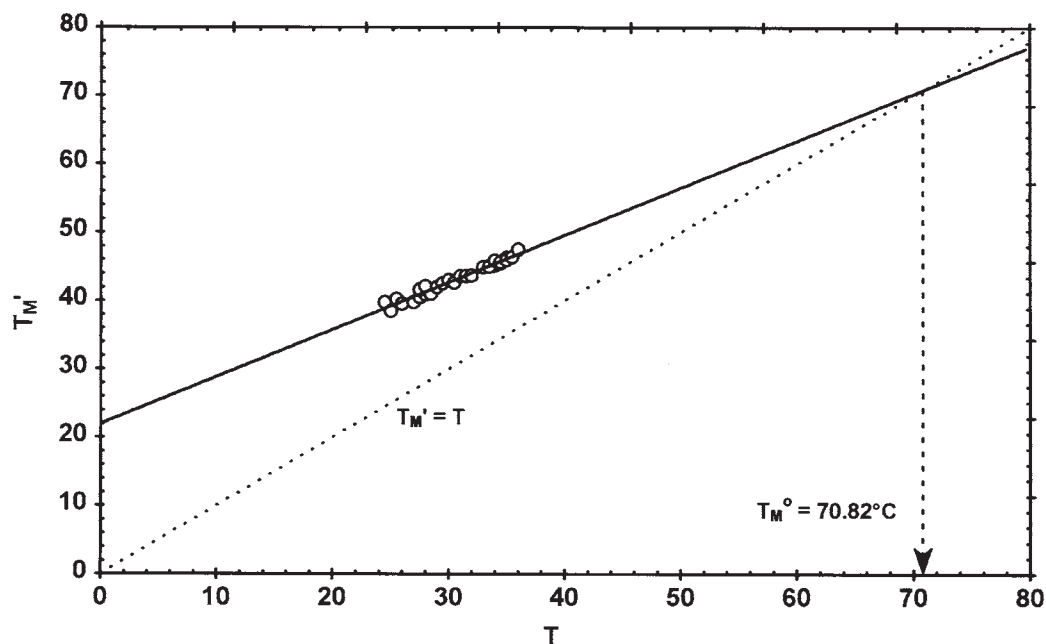


FIG. 2. Determination of the equilibrium melting temperature, T_M^o , for palm stearin crystallization in sesame oil. T is the isothermal crystallization temperature and T_M' is the apparent melting temperature of the tripalmitin peak in the blends of palm stearin in sesame oil determined in the melting differential scanning calorimetry (DSC) thermograms (see Figs. 12 and 13).

TABLE 1
Fatty Acid Profile^a for Sesame Seed Oil and Palm Stearin (% wt/vol)

Fatty acid	Sesame oil			Palm stearin
	Present study	Ref. 9	Ref. 1	
Palmitic	9.87 ± 0.18	10.03 ± 0.21	9.35 ± 0.23	51.88 ± 1.88
Stearic	5.66 ± 0.05	5.71 ± 0.05	6.10 ± 0.37	4.67 ± 0.09
Palmitoleic	0.23 ± 0.04	0.28 ± 0.05	0.18 ± 0.04	ND ^b
Oleic	40.25 ± 0.21	40.14 ± 0.20	42.75 ± 1.14	33.66 ± 1.44
Linoleic	43.16 ± 0.14	42.70 ± 0.12	39.70 ± 1.28	8.05 ± 0.58
Linolenic	0.24 ± 0.01	0.61 ± 0.15	0.58 ± 0.04	0.42 ± 0.02
<i>Cis</i> -Vaccenic	ND	ND	0.85 ± 0.05	ND
Arachidic	ND	ND	0.30 ± 0.00	ND
Unknown	0.58 ± 0.05	0.64 ± 0.15	ND	1.37 ± 0.06

^aMean ± standard deviation ($n = 4$). ND, not determined.

the sesame seed oil thermograms were similar to the ones reported in our previous study (8), small differences in peak temperatures were observed. These differences mainly arise from the variation in the fatty acid composition between the sesame oils utilized in each study (Table 1) and from differences in the calibration procedure used in the DSC. In this study, a two-point (i.e., indium and *n*-hexatriacontane) temperature calibration was used, whereas in our previous report (8), a one-point (i.e., indium) calibration was performed. Therefore, the results reported here are more accurate.

The cooling thermogram for PS was quite simple with two crystallization peaks with maxima at 298.7 and 275.5 K, which corresponded to the highly saturated and unsaturated (i.e., olein fraction) triglyceride fractions, respectively (14,21). Based on the thermal and X-ray analysis of Busfield and Proschogo (26) and Swe *et al.* (27), the high-temperature endothermic peaks during the heating thermogram for PS were assigned to poly-

morphic states β_1' ($T_p = 311.1$ K) and β_1 ($T_p = 324.1$ K) (Fig. 4), while the low-temperature melting peak to polymorph states β_2' ($T_p = 275.8$ K) and α ($T_p = 281.1$). The β' crystal's size and shape produces good spreadability and plasticity to margarines and shortenings, since a fine crystal network is formed. However, some fats undergo a β' to β polymorph state transformation, which is induced by temperature fluctuations during storage. This results in products with hard consistency and sandy texture, since β crystals are bigger than β' crystals and have a higher melting temperature (8,28). Fats with high levels of C_{48} and C_{54} triglycerides are prone to β formation of crystals (i.e., PPP, OOO, StOSt, StStSt), as in hydrogenated canola and sunflower oils. In contrast, C_{50} (i.e., PPSt, PPO) and C_{52} (i.e., POSt) triglycerides are strong β' formers (28), which explains the beneficial effect of palm oil and its derivatives (e.g., PS) in margarines and shortenings (29).

From the studies of Che Man *et al.* (14), and from experi-

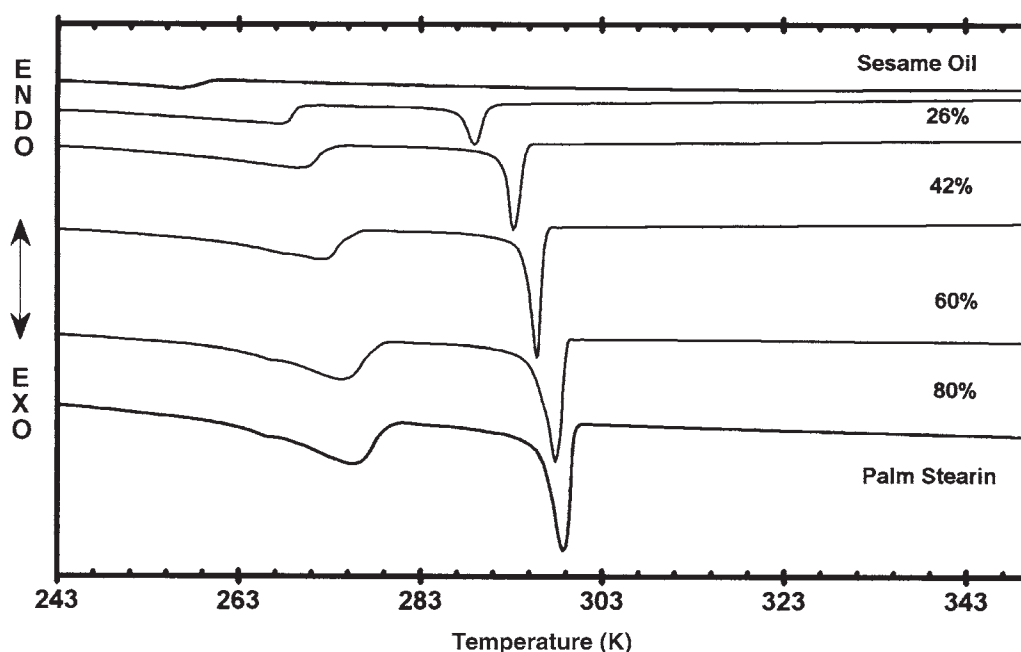


FIG. 3. Dynamic cooling thermogram (10 K/min) for sesame oil, palm stearin, and blends of palm stearin in sesame oil at different proportion.

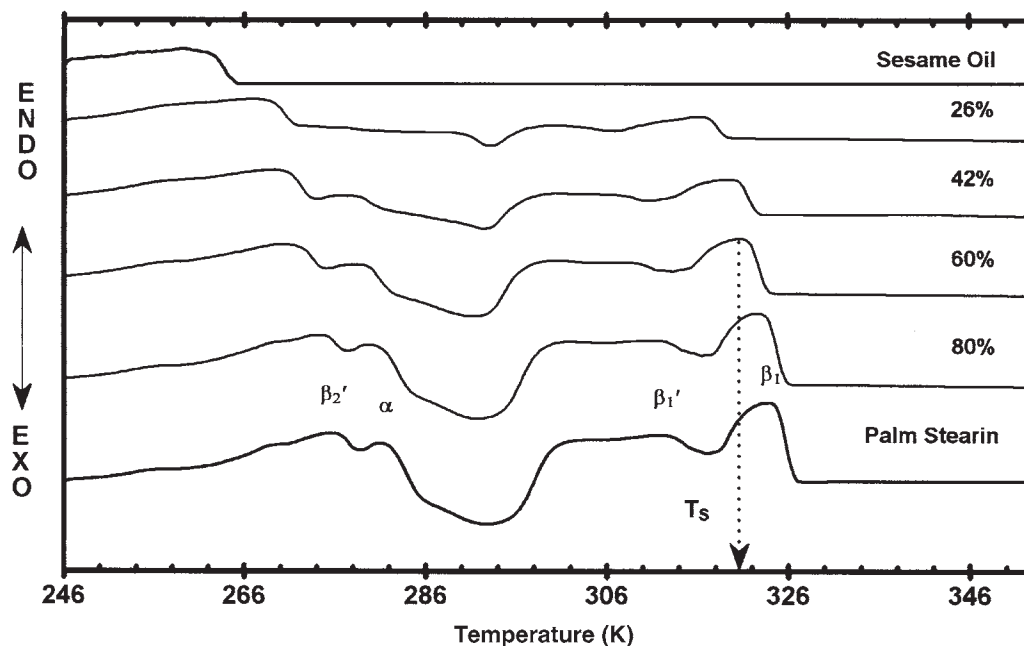


FIG. 4. Dynamic heating thermograms (5 K/min) for sesame oil, palm stearin, and blends of palm stearin in sesame oil at different proportion. T_s is the melting temperature of the tripalmitin peak. The polymorph states assigned to each endothermic peak are shown.

mental studies that involved the addition of pure TP to PS and PS/sesame oil solutions and further determination by DSC of the corresponding ΔH for crystallization and melting (data not shown), we established that the exotherm at 298.7 K corresponded to TP crystallization. The position of this peak shifted

to a lower temperature and broadened as PS was diluted with sesame oil (Fig. 3). As well, the melting events corresponding to the polymorphic states of the high- and low-temperature peaks (i.e., β_1' and β_1 , β_2' , and α , respectively), shifted to lower temperature and broadened as PS concentration decreased in

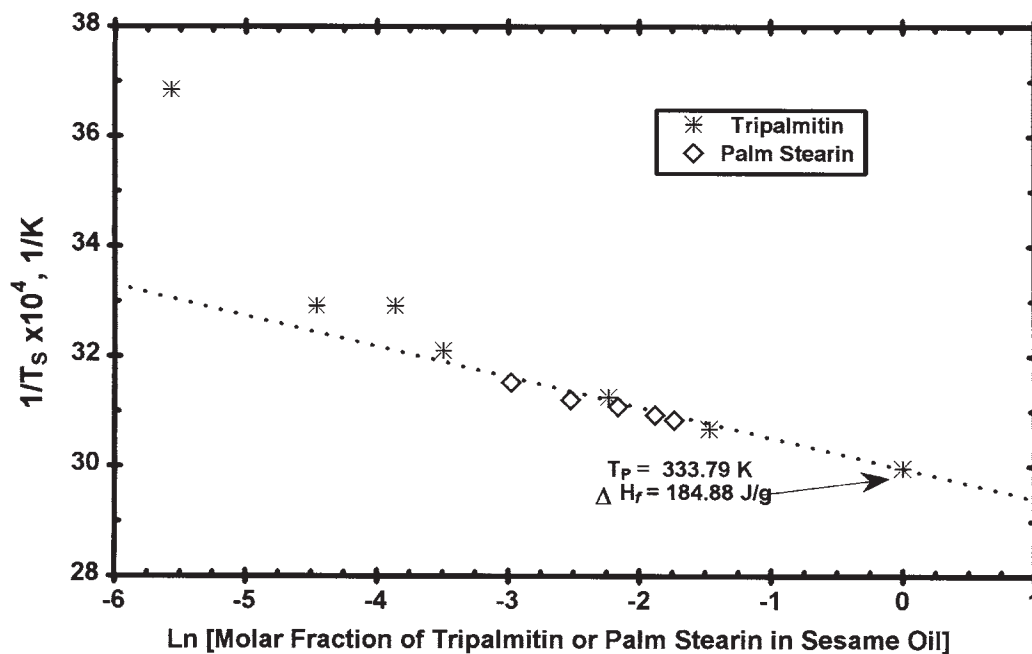


FIG. 5. Hildebrand plot for the blends of pure tripalmitin in sesame oil (0.32, 0.98, 1.80, 2.62, 10, and 25% wt/vol) and palm stearin in sesame oil (26, 42, 60, 80, and 100% wt/vol). T_P and ΔH_f are the experimental melting temperature and the molar enthalpy of fusion for pure tripalmitin, respectively.

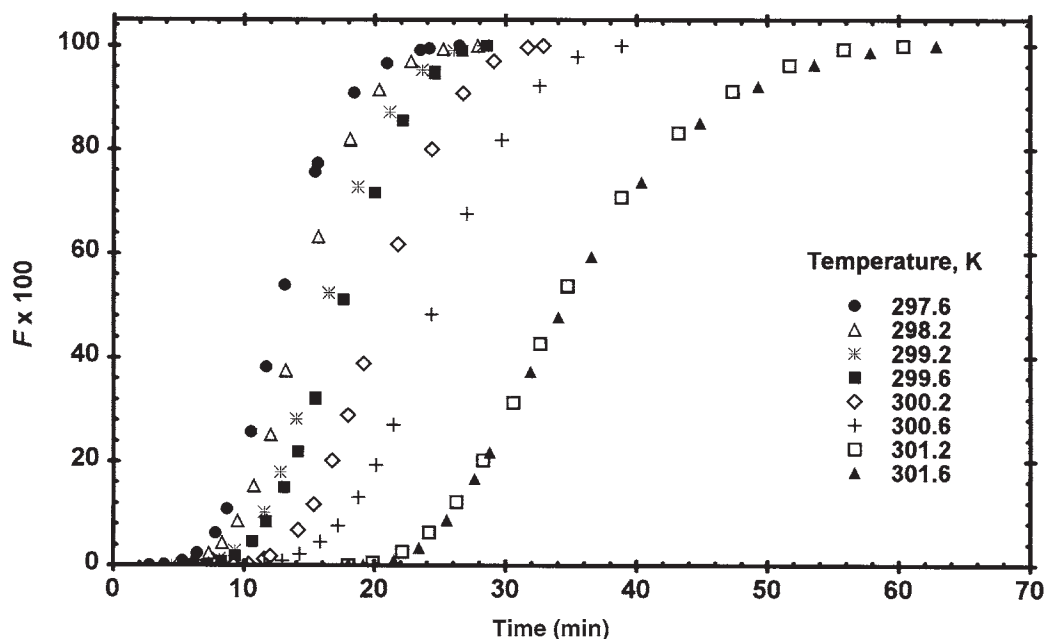


FIG. 6. Percentage of reduced crystallinity ($F \times 100$) as a function of time at different temperatures in the 26% palm stearin blend in sesame oil.

the blends (Fig. 4). The same trends were observed in solutions of pure TP in sesame oil (8), and this behavior was associated with solubility of TP in sesame oil. This can be appreciated in Figure 5, since our crystallization and melting data for the PS/sesame oil system fitted the Hildebrand equation very well. This relationship was also investigated for the TP/sesame oil system, also obtaining good agreement with the Hildebrand model as long as the TP concentration was higher than 0.98%. As indicated by Dibildox-Alvarado and Toro-Vazquez (8), at TP concentration lower than 0.98%, a high-melting-temperature triglyceride fraction of sesame oil could co-crystallize with TP and depress the melting point below the value predicted for pure TP. Then, within the concentrations of PS utilized in the sesame oil solutions, the fully saturated triglyceride fraction from PS (i.e., mainly TP) crystallized independently from sesame oil. Using reduced viscosity measurements in solutions of TP or tristearin in sesame oil, Toro-Vazquez and Gallegos-Infante (15) have shown that, prior to crystal nucleation, saturated triglycerides are segregated from the original lamellar organization of the unsaturated triglycerides in sesame oil.

The experimental T_p value for pure TP was 333.79 K with a ΔH_f of 184.88 J/g. These values are somewhat different from the ones determined previously by our group (8) under similar heating and cooling conditions ($T_p = 342$ K, $\Delta H_f = 185.37$ J/g) and by Norton's group (30) at a heating rate of 0.125 K/min ($T_p = 339.7$ K, $\Delta H_f = 204.37$ J/g). These differences might arise mainly for two reasons. First, as previously mentioned, a two-point calibration was used in the present study, whereas in previous reports (8,30) a one-point calibration was performed. In consequence, the results reported here are more accurate. Second, the shape of melting/crystallization curves and the behavior of polymorphic transformations are strongly affected by the

TABLE 2

Free Energy for Nucleation (ΔG_c) Index of Avrami (n), and Crystallization Rate Constant (z) for Palm Stearin Crystallization in Sesame Oil as a Function of Crystallization Temperature

Crystallization temperature (K)	Palm stearin (% wt/vol)	ΔG_c (kJ/mol)	Avrami parameters	
			n	$z \times 10^{-8}$ (min^{-1})
297.6	26	11.97	4.4	821.95
298.2		12.24	4.7	249.56
299.2		12.79	4.8	109.69
299.6		13.08	4.6	131.06
300.2		13.38	5.4	5.91
300.6		13.69	5.5	1.31
301.2		14.01	5.1	1.14
301.6		14.34	4.5	7.40
300.6	42	9.75	4.3	3095.43
301.2		9.98	4.0	5858.69
302.2		10.46	4.4	649.16
302.6		10.72	4.8	197.29
303.2		10.98	4.7	120.14
303.6		10.26	5.0	9.86
304.2		11.54	5.0	2.81
304.6		11.83	5.2	0.85
304.6	60	9.12	5.4	53.34
305.2		9.36	4.8	81.83
306.2		9.86	5.3	19.72
306.6		10.13	5.5	1.18
307.2		10.40	3.9	44.46
307.6		10.69	4.6	1.88
308.2		10.99	4.1	11.64
306.2	80	6.29	5.3	30.10
306.6		6.46	4.8	57.38
307.2		6.64	5.0	55.85
307.6		6.82	5.0	15.18
308.2		28.04	5.5	3.87
308.6		28.84	4.7	3.51
309.2		29.67	5.3	0.03

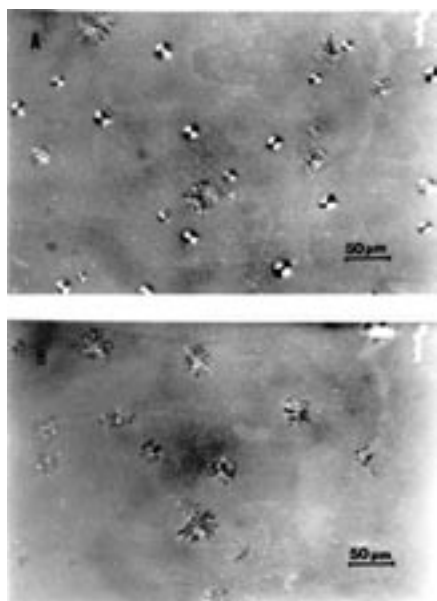


FIG. 7. Polarized light microphotographs of the crystals obtained with the 26% palm stearin (PS)/sesame oil solution at 297.6 K (6 min after τ_i , A) and 299.2 K (6.5 min after τ_i , B). τ_i , induction time of crystallization.

scan rate used during the DSC analysis (30). The Hildebrand equation obtained by linear regression using the experimental data for the 26, 42, 60, and 80% PS/sesame oil solutions [$1/T_g = 29.918 \times 10^{-4} - \ln(\text{molar fraction of PS in sesame oil})(0.531 \times 10^{-4})$] provided predictions for TP of $T_p = 334.25$ K and $\Delta H_f = 185.92$ J/g. These values are quite similar to the ones obtained experimentally by DSC measurements for pure TP.

The plot of the percentage of reduced crystallinity, $F \times 100$, as a function of time for the different PS/sesame oil solutions followed the same general behavior as shown for the 26% PS blend in Figure 6, i.e., increasing the rate of crystallization beyond the value of τ_i and then decreasing it until achieving zero crystallization rate at $F \times 100 = 100$. The values of n and z , the index of Avrami and the rate constant of crystallization, respectively, as a function of the crystallization temperature are shown in Table 2. A regression coefficient greater than 0.998 was always obtained for the linear regression of $\ln[-\ln(1 - F)]$ on $\ln(t)$. The coefficient of variation for replicate measurements was less than 6% for calculation of n and less than 8% for calculation of z . Values of n around 4 or greater were obtained in all cases. Similar magnitudes have been obtained by Metin and Hartel (31) in blends of cocoa butter with 5 and 10% of anhydrous milk fat (AMF) or solid fractions of AMF obtained by crystallization at 23, 28, 30, or 32°C. On the other hand, Kawamura (19) obtained values of n around 4 in palm oil crystallization. Based on the theory of crystallization of Avrami (18), values of n greater than 4 suggest heterogeneous nucleation and indicate the effect of sporadic nucleation on the development of new crystals. However, additional considerations associated with the effect of the cooling rate on the local-order (i.e., triglyceride lamellar organization), sporadic nucleation, and secondary crystallization must be taken into account in the determination of n values of triacylglyceride crystallization (Toro-Vazquez, J.F., Herrera-Coronda, V., Dibiddox-Alvarado, E., and Char'o-Alonso, N., unpublished results). Figures 7–9 are microphotographs of crystals developed in the 26% and 80% PS/sesame oil solution at different temperatures and crystallization time after the induction of crystallization (τ_i). TP is

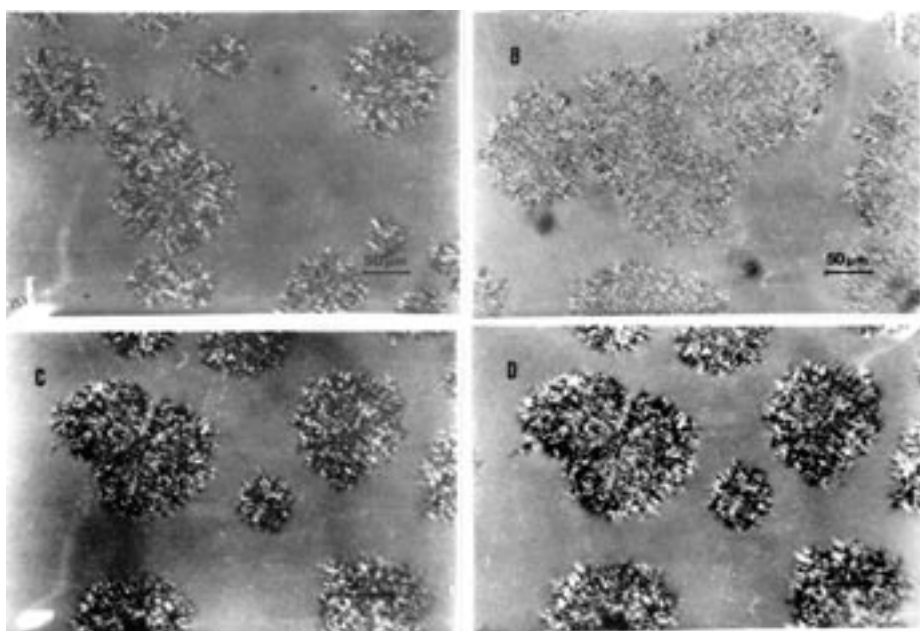


FIG. 8. Polarized light microphotographs of the crystals obtained with the 80% PS/sesame oil solution at 306.2 K (12 min and 20 min after τ_i , A and B, respectively) and 307.2 K (14 min and 20 min after τ_i , C and D, respectively). For abbreviations see Figure 7.

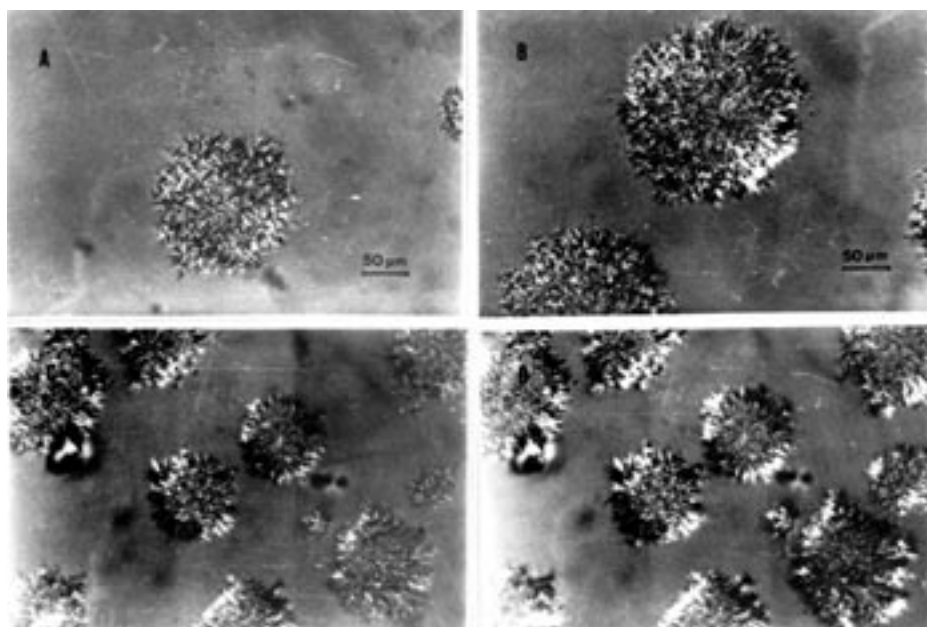


FIG. 9. Polarized light microphotographs of the crystals obtained with the 80% PS/sesame oil solution at 308.2 K (12 min and 20 min after τ_i , A and B, respectively) and 309.2 K (12 min and 20 min after τ_i , C and D, respectively). For abbreviations see Figure 7.

the triglyceride with the highest melting temperature in the PS/sesame oil system (28); however, once it crystallizes under isothermal conditions, it may promote the crystallization (e.g., heterogeneous crystallization) of other triglycerides with lower melting points (i.e., PPSt, POSt, and PPO). In blends of sesame oil with TP, values of n between 2 and 4 have been obtained (8). However, in that study pure TP was used. Additionally, the

crystallization process was followed through transmittance measurements, and crystal birefringence might have affected the transmittance values modifying the crystallization curve in comparison with the one obtained by DSC. In polymer crystallization, Avrami crystallization curves determined by DSC provide different information and n values than the ones obtained by transmitted polarized light microscopy (32). Since hetero-

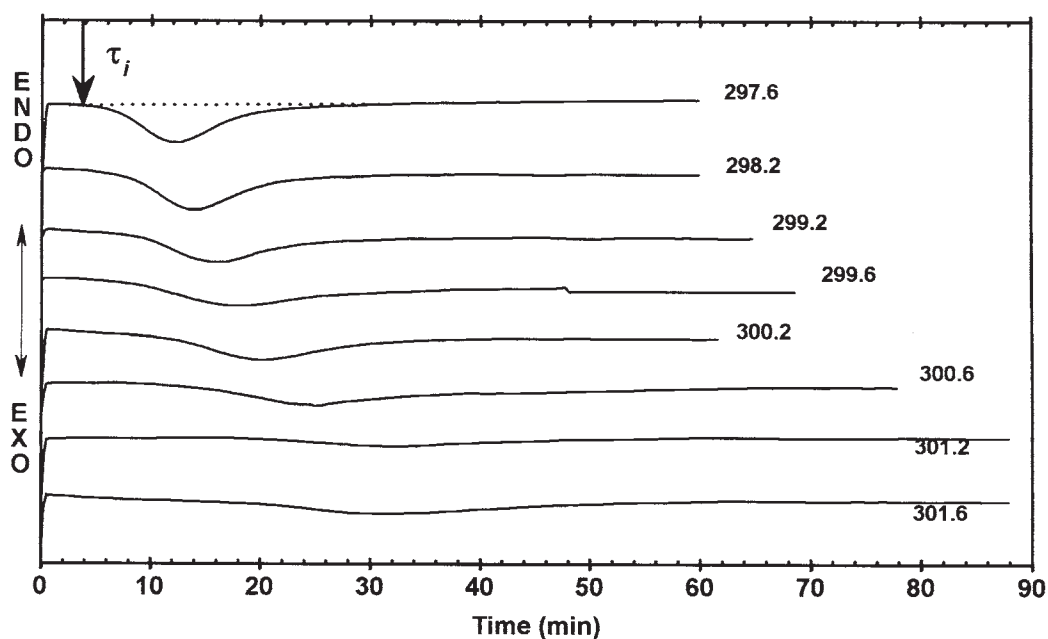


FIG. 10. DSC isothermal profile for the 26% PS in sesame oil at different temperatures. The induction time for crystallization (τ_i) is shown for a given temperature. For abbreviation, see Figure 2.

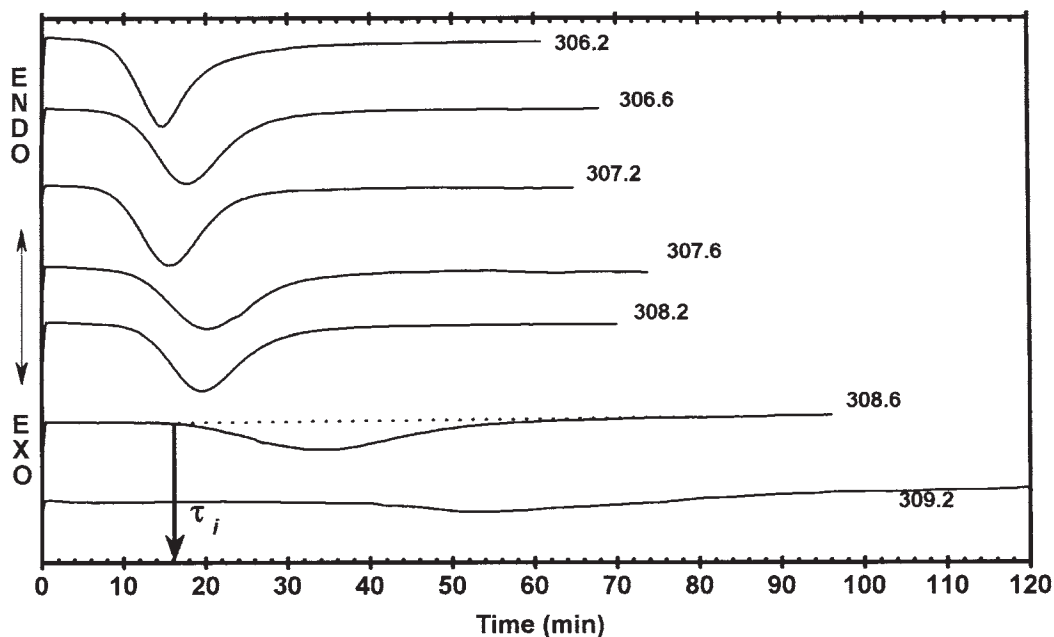


FIG. 11. DSC isothermal profile for the 80% PS in sesame oil at different temperatures. The induction time for crystallization (τ_i) is shown for a given temperature. For abbreviations see Figures 2 and 10.

geneous nucleation, sporadic nucleation, and secondary crystallization are more prevalent as crystallization time goes on, the intrinsic birefringence of crystals is not constant with time. This is evident from microphotographs in Figures 8 and 9. As a result, events like heterogenous nucleation and secondary crystallization might be more evident with the measurement of transmitted light than with DSC.

Figures 10 and 11 show the isothermal DSC profiles (i.e., isothermal crystallization) for the 26 and 80% PS/sesame oil solutions. In palm oil, two exotherms, I and II in order of generation, were obtained under isothermal conditions at temperatures lower than 297 K; at temperatures of 299 K or higher, peak I disappeared (19). In the present study only one exotherm of crystallization was obtained in all cases. The corresponding

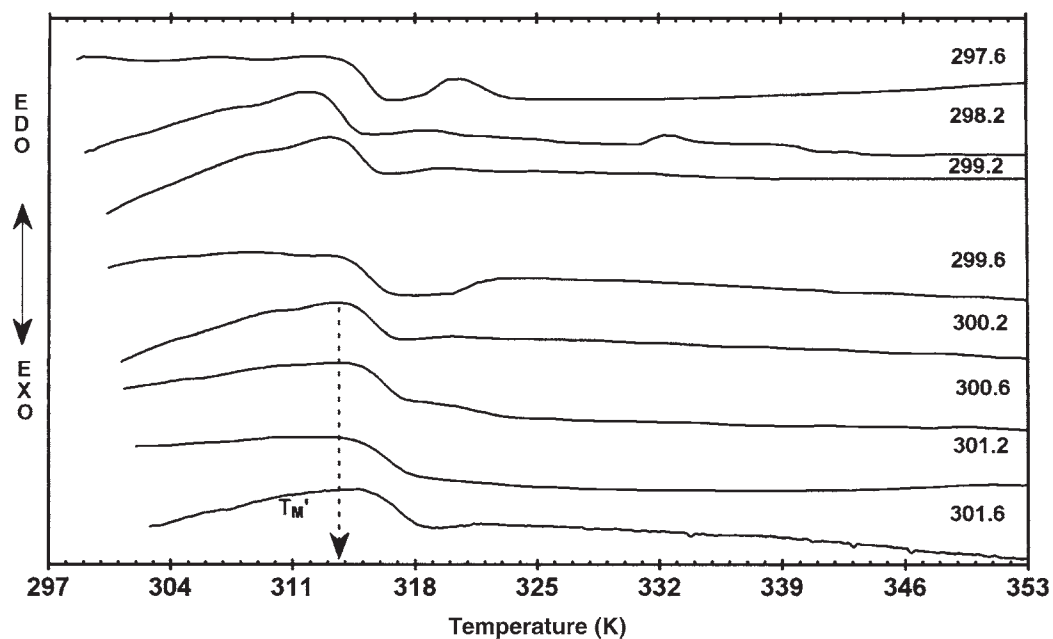


FIG. 12. Melting profile for crystals obtained in the 26% PS blend in sesame oil according to the conditions shown in Figure 7. For abbreviation see Figure 7.

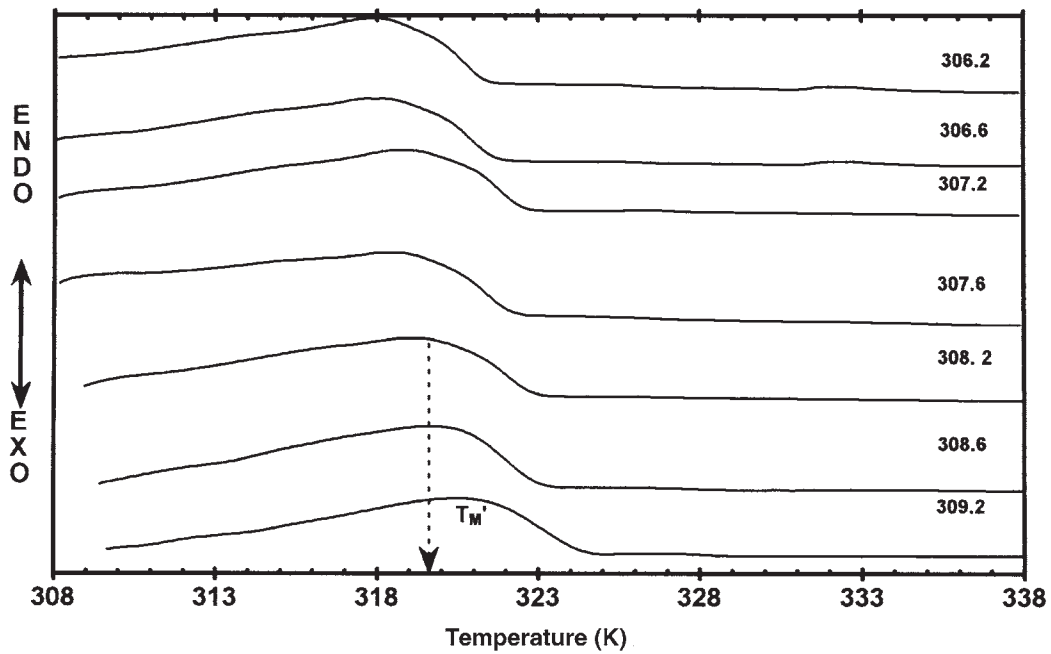


FIG. 13. Melting profile for crystals obtained in the 80% PS blend in sesame oil according to the conditions shown in Figure 8. For abbreviation see Figures 2 and 7.

melting profile of the crystals showed a major endothermic peak, with melting completed at temperatures lower than 320 K in the 26 (Fig. 12) and 42% blends (data not shown), and at temperatures lower than 324 K in the 60 (data not shown) and 80% blends (Fig. 13). The melting peak temperature associated with this endotherm was utilized as T_M' to establish the magni-

tude of τ_M^o (Figs. 12 and 13). Additional endothermic peaks of smaller size also were observed, which were related with melting events at higher temperatures. These peaks were more apparent at lower temperature of crystallization and thus were more apparent in the 26% PS/sesame oil solution than in the rest of the blends (Figs. 12 and 13). Based on the investigations

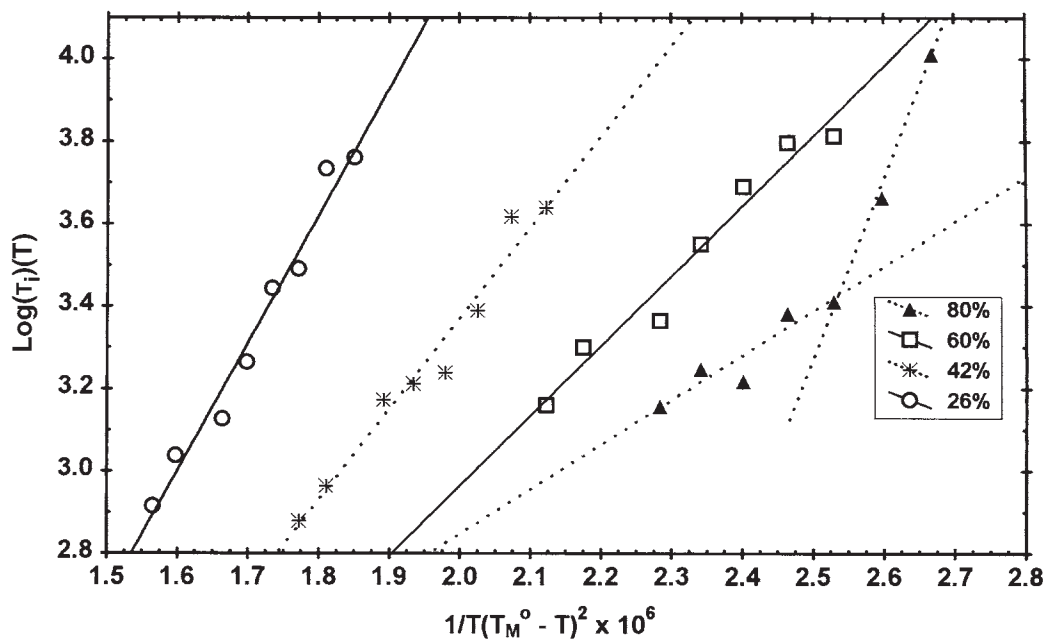


FIG. 14. Fitting of the nucleation kinetics of PS blends in sesame oil according to the Fisher-Turnbull equation. For abbreviations see Figures 2 and 7.

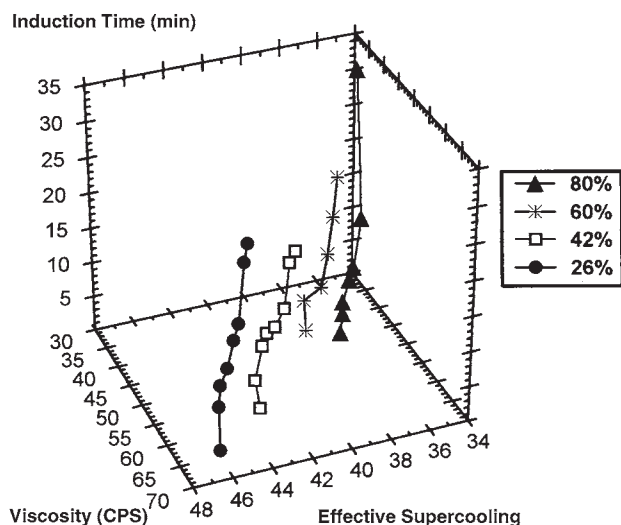


FIG. 15. Association among the induction time for crystallization, viscosity of the oil phase, and effective supercooling for the PS blends in sesame oil. See Figure 7 for abbreviation.

of Kawamura (19,33), the results indicate that the crystallization peak obtained in the 26, 42, and 60% PS/sesame oil solutions corresponded to β_1' crystals, probably mixed with α crystals. The proportion of α to β_1' depended on the temperature of crystallization; thus, the lower the crystallization temperature the more α crystals were present, decreasing the melting temperature of the major endothermic peak. On the other hand, the minor melting peaks observed in the heating thermograms of the crystals obtained at the lower crystallization temperatures (i.e., $T \leq 300.2$ K, Fig. 12) were associated with β_1 crystals. These crystals probably developed through a polymorph transformation from α crystals, the earlier transition to β_1' crystals occurring at the beginning of the isothermal crystallization (32). However, as the temperature of crystallization increased in the 26, 42, and 60% PS/sesame oil solution, β_1' crystallization predominated over α , and no $\alpha \rightarrow \beta_1' \rightarrow \beta_1$ transformation occurred (i.e., $T \geq 300.6$ K, Fig. 12). Since these minor peaks were derived from a polymorph transformation, they were not considered in the determination of T_M^o . The microphotographs shown in Figure 7 support these observations since at $T = 297.6$ K, the lower crystallization temperature utilized with the 26% PS/sesame oil solution, two different types of crystals developed (i.e., β_1' crystals mixed with α crystals) (Fig. 7A). When the crystallization temperature was increased to 299.2 K, just one type of crystal was developed (i.e., β_1' crystallization predominated over α) (Fig. 7B). In contrast, in the 80% PS/sesame oil solution, where in general higher crystallization temperatures were used (Fig. 11), the crystals obtained at $T \leq 307.6$ K were associated with the β_1' polymorph state (Fig. 8) while crystals developed at $T \geq 308.2$ K crystallized in the β_1 polymorph state (Fig. 9). The fitting of the nucleation kinetics of PS in sesame seed oil to the Fisher-Turnbull equation (Fig. 14) supported these observations. Thus, a good linearity was observed within the effective supercooling interval investigated

($r > 0.98$, $P < 0.0001$) for the 26, 42, and 60% PS/sesame oil solutions. However, with the 80% PS/sesame oil solution a discontinuity in the plot was evident around 307 K. This behavior showed that within the interval of effective supercooling investigated, the 26, 42, and 60% PS/sesame oil solutions crystallized mainly in a particular polymorph state (i.e., β_1' mixed with some α particularly at very low supercooling, Fig. 7A), while the 80% solution crystallized in two different polymorph states (i.e., β_1' at $T \leq 307.6$ K and β_1 at $T \geq 308.2$ K, Figs. 8 and 9).

The ΔG_c values for the PS/sesame oil solutions as a function of the crystallization temperature are shown in Table 2. Lower ΔG_c values have been obtained for palm oil, PS (21), and hydrogenated sunflower oil (22). In these studies a relative supercooling (i.e., $T_s - T$) rather than the effective supercooling (i.e., $T_M^o - T$) was utilized in the calculation of ΔG_c (Eqs. 4 and 5) since the value of T_M^o was not established. Formal studies that evaluate the effect of supercooling require the determination of T_M^o (23,34). From the results in Table 2, it is evident that as the temperature of crystallization increases and the PS is more diluted in sesame oil, PS crystallization is more difficult (i.e., ΔG_c increases). A particular case represented the β_1 crystallization (i.e., 80% PS at $T \geq 308.2$ K) since its ΔG_c values indicated a significantly more difficult nucleation than the β_1' polymorph. Our data showed that in spite of the higher concentrations of PS in the 80% PS/sesame oil system, crystallization in the β_1 state required more energy for its development than β_1' crystallization in the 26, 42, and 60% PS/sesame oil.

As we mentioned earlier, the rate of nucleation from the melt, J , depends on both ΔG_c and the activation free energy for molecular diffusion, ΔG_d . The viscosity is a physical parameter inversely proportional to molecular diffusion. Thus, the effect of the viscosity of the oil phase on τ_i , as a function of the effective supercooling is shown in Figure 15. Overall, the effective supercooling was higher for the 26 and 42% PS solutions and lower for the 60 and 80% PS solutions. For a particular PS solution the increment in the effective supercooling produced a higher viscosity of the oil phase and a decrease in the τ_i (Fig. 15). This behavior has the following explanation. Under the supercooling conditions investigated and at the low cooling rate used (i.e., 1 K/min), triglyceride molecules have enough time to organize in the liquid state in lamellar structures (see Ref. 9) while the temperature decreases. As a result, an increase in viscosity is observed. Thus, once isothermal conditions have been achieved, the lamellar structures of the triglycerides further organize and achieve a critical size to develop a stable nucleus. This last process will take place in shorter time (i.e., smaller τ_i) the longer the system takes to achieve isothermal conditions (i.e., the higher the effective supercooling). Further increments in the effective supercooling (e.g., lowering even more the crystallization temperature) resulted in crystallization even before achieving the corresponding isothermal temperature. Non-isothermal crystallization follows different kinetics (15) and was not evaluated in the present investigation.

It is generally accepted that molecular diffusion decreases with decreasing temperature. Thus, as effective supercooling increases, the crystal size resulting from crystallization must

decrease. In fact, this has been shown in TP crystallization in sesame oil using measurements of relative supercooling (i.e., $T_s - T$) and the crystallization rate constant (z , Eq. 2) (35). The β_1' (and α) crystals from PS, developed at the highest effective supercooling investigated (Fig. 7), were smaller than the β_1 crystals obtained in the 80% PS solution at the lower effective supercooling (Fig. 9). In general, β' form and small size confer a fine crystal network that incorporates large amounts of liquid oil and provides good spreadability and plasticity to margarines, shortenings, and vegetable spreads (29). In contrast, β form, larger size, and higher melting temperature than β' crystals provide a sensation of sandiness and a dull appearance to margarines and spreads (29).

From the above, the occurrence of a $\beta' \rightarrow \beta$ polymorphic transition is important to establish the functionality of PS in blends with sesame oil to produce value-added products like margarines and, overall, vegetable spreads. Gibon *et al.* (25) showed that the β' state of PPP is less prone to the $\beta' \rightarrow \beta$ polymorphic transition when crystallized directly from the melt (i.e., PS/sesame oil solution) than when occurring through the process $\alpha \rightarrow \beta' \rightarrow \beta$. According to the authors this phenomenon is due to a better "crystalline perfection" of the β' lattice obtained directly and slowly modified from the melt. The processing conditions to achieve a stable β' state must be established in the PS/sesame oil solutions to produce products acceptable to the consumers. One limiting aspect regarding the use of PS in blends with sesame oil is the consumer concern regarding the cholesterol-raising effect of saturated (i.e., palmitic acid) fatty acids. However, the positional distribution of palmitic acid in palm oil is predominantly in the *sn*-1 and *sn*-3 positions of the triglycerols, whereas in animal fats palmitic acid occupies mainly the *sn*-2 position. This difference in the positional distribution of palmitic acid in the triglycerols might account for the thrombogenic effect observed in animal fats which is not significantly present when palm oil or its derivatives are consumed by rats or humans (36,37).

ACKNOWLEDGMENTS

The present work was supported by CONACYT through the grant #485100-5-28251B.

REFERENCES

- Kamal-Eldin, A., and L.Å. Appelqvist, Variation in Fatty Acid Composition of the Different Acyl Lipids in Seed Oils from Four *Sesamum* Species, *J. Am. Oil Chem. Soc.* 71:135–139 (1994).
- Salunkhe, D.K., J.K. Chavan, R.N. Adsule, and S.S. Kadam, Sesame, in *World Oilseeds: Chemistry, Technology and Utilization*, Van Nostrand Reinhold, New York, 1991, pp. 371–402.
- Kamal-Eldin, A., and L.Å. Appelqvist, Variation in Composition of Sterols, Tocopherols and Lignans in Seed Oils from Four *Sesamum* Species, *J. Am. Oil Chem. Soc.* 71:149–156 (1994).
- Kamal-Eldin, A., L.Å. Appelqvist, and G. Yousif, Lignan Analysis in Seed Oils from Four *Sesamum* Species: Comparison of Different Chromatographic Methods, *Ibid.* 71:141–147 (1994).
- About-Gharbia, H.A., F. Shahidi, A.A.Y. Shehata, and M.M. Youssef, Oxidative Stability of Extracted Sesame Oil from Raw and Processed Seeds, *J. Food Lipids* 3:59–72 (1996).
- Yoshida, H., and G. Kajimoto, Microwave Heating Affects Composition and Oxidative Stability of Sesame (*Sesamum indicum*) Oil, *J. Food Sci.* 59:613–616 (1994).
- Shahidi, F., R. Amarowicz, H.A. Abou-Gharbia, and A.Y. Shehata, Endogenous Antioxidants and Stability of Sesame Oil as Affected by Processing and Storage, *J. Am. Oil Chem. Soc.* 74:143–148 (1997).
- Dibildox-Alvarado E., and J. Toro-Vazquez, Isothermal Crystallization of Tripalmitin in Sesame Oil, *Ibid.* 74:69–76 (1997).
- Toro-Vazquez, J.F., and M. Charó-Alonso, Physicochemical Aspects of Triacylglycerides and Their Association to Functional Properties of Vegetable Oils, in *Functional Properties of Proteins and Lipids, ACS Symposium Series 70*, edited by J.R. Whitaker, F. Shahidi, A. López Munguía, R.Y. Yada, and G. Fuller, American Chemical Society, Washington, DC, 1998, pp. 230–253.
- Haumann, B.F., Widening Array of Spreads Awaits Shoppers, *INFORM* 9:6–13 (1998).
- Haumann, B.F., Tools: Hydrogenation, Interesterification, *Ibid.* 5:668–678 (1994).
- Hamm, W., Trends in Edible Oil Fractionation, *Trends Food Sci. Technol.* 6: 121–126 (1995).
- Yusoff, M.S.A., H. Kifli, H.D.M. Noor Lida, and M.P. Rozie, (1998) The Formulation of *Trans* Fatty Acid-Free Margarines, in *Emerging Technologies, Current Practices, Quality Control, Technology Transfer, and Environmental Issues*, Vol. 1, edited by S.S. Koseoglu, K.C. Rhee, and R.F. Wilson, AOCS Press, Champaign, 1998, pp. 156–158.
- Che Man, Y.B., T. Haryati, H.M. Ghazali, and B.A. Asbi, Composition and Thermal Profile of Crude Palm Oil and Its Products, *J. Am. Oil Chem. Soc.* 76:237–242 (1999).
- Toro-Vazquez, J.F., and A. Gallegos-Infante, Viscosity and Its Relationship to Crystallization in a Binary System of Saturated Triacylglycerides and Sesame Seed Oil, *Ibid.* 73:1237–1246 (1996).
- Nikolova-Damyanova, N., Silver Ion Chromatography and Lipids, in *Advances in Lipid Methodology—One*, edited by W.W. Christie, The Oily Press, Glasgow, 1992, pp. 181–237.
- Hildebrand, J.H., and S.R. Scott, *Solubility of Nonelectrolytes*, 3rd edn., Reinhold Publishing Corporation, New York, 1950.
- Avrami, M., Kinetics of Phase Change. II. Transformation–Time Relations for Random Distribution of Nuclei, *J. Chem. Phys.* 8:212–224 (1940).
- Kawamura, K., The DSC Thermal Analysis of Crystallization Behavior in Palm Oil, *J. Am. Oil Chem. Soc.* 56:753–758 (1979).
- Henderson, D.W., Thermal Analysis of Non-Isothermal Crystallization Kinetics in Glass Forming Liquids, *J. Non-Crystalline Solids* 30:301–305 (1979).
- Ng, W.L., A Study of the Kinetics of Nucleation in a Palm Oil Melt, *J. Am. Oil Chem. Soc.* 67:879–882 (1990).
- Herrera, M.L., C. Falabella, M. Melgarejo, and M.C. Añon, Isothermal Crystallization of Hydrogenated Sunflower Oil: I—Nucleation, *Ibid.* 75:1273–1280 (1998).
- Hoffman, J.D., and J.J. Weeks, Melting Process and the Equilibrium Melting Temperature of Polychlorotrifluoroethylene, *J. Res. Nat. Bur. Std.* 66:13–28 (1962).
- Hoffman, J.D., and J.J. Weeks, Rate of Spherulitic Crystallization with Chain Folds in Polychlorotrifluoroethylene, *Chem. Phys.* 37:1723–1733 (1962).
- Gibon, V., F. Durant, and Cl. Deroanne, Polymorphism and Intersolubility of Some Palmitic, Stearic and Oleic Triglycerides: PPP, PSP, POP, *J. Am. Oil Chem. Soc.* 63:1047–1055 (1986).
- Busfield, W.K., and P.N. Proschogo, Thermal Analysis of Palm Stearin by DSC, *Ibid.* 67:171–175 (1990).

27. Swe, P.Z., Y.B. Che Man, and H.M. Ghazali, Polymorphic Study of High Melting Glycerides of Palm Olein Crystals, *Mal. Oil Sci. Tech.* 4:205–208 (1995).
28. deMan, J.M., Functionality of Palm Oil in Foods, *J. Food Lipids* 5:159–170 (1998).
29. deMan, J.M., and L. deMan, Palm Oil as a Component for High Quality Margarine and Shortening Formulations, *Mal. Oil Sci. Tech.* 4:56–60 (1995).
30. Norton, I.T., C.D. Lee-Tuffnell, S. Ablett, and S.M. Bociek, Calorimetric, NMR and X-ray Diffraction Study of the Melting Behavior of Tripalmitin and Tristearin and Their Mixing Behavior with Triolein, *J. Am. Oil Chem. Soc.* 62:1237–1244 (1985).
31. Metin, S., and R.W. Hartel, Thermal Analysis of Isothermal Crystallization Kinetics in Blends of Cocoa Butter with Milk Fat or Milk Fat Fractions, *Ibid.* 75:1617–1624 (1990).
32. Medellín-Rodríguez, F.J., and P.J. Phillips, Poly(aryl ether ketone) (PEEK) (Bulk Crystallization), *Polym. Materials Enc.* 75:5513–5518 (1996).
33. Kawamura, K., The DSC Thermal Analysis of Crystallization Behavior in Palm Oil. II, *J. Am. Oil Chem. Soc.* 57:48–52 (1980).
34. Colomer Vilanova, P., S. Monsellat Ribas, and G. Martín Guzmán, Isothermal Crystallization of Poly(ethylene-terephthalate) of Low Molecular Weight by Differential Scanning Calorimetry: 1. Crystallization Kinetics, *Polymer* 26:423–428.
35. Dibildox-Alvarado, E., and J.F. Toro-Vazquez, Evaluation of Crystallization in Sesame Oil Through a Modified Avrami Equation, *J. Am. Oil Chem. Soc.* 75:73–76 (1998).
36. Renaud, S.C., J.C. Ruf, and D. Petithory, The Positional Distribution of Fatty Acids in Palm Oil and Lard Influences Their Biological Effects in Rats, *J. Nutr.* 125:229–237 (1995).
37. Zock, P.L., J.H.M. Vries, N.J. Foom, and M.B. Katan, Positional Distribution of Fatty Acids in Dietary Triglycerides: Effects on Fasting Blood Lipoprotein Concentrations in Humans, *Am. J. Clin. Nutr.* 61:48–55 (1995).

[Received May 5, 1999; accepted December 5, 1999]